

STABILITY ANALYSIS OF A FRACTIONAL ORDER CORONAVIRUS(COVID-19) EPIDEMIC MODEL

M. KHUDDUSH^{1*}, K. R. PRASAD², §

ABSTRACT. In this paper a six-compartmental coronavirus(COVID-19) epidemic model is developed. We have divided the total population into five classes, namely susceptible, exposed, infected, treatment, recovered and the concentration of the coronavirus in the environment reservoir class. The basic reproduction number \mathcal{R}_0 is calculated using the next-generation matrix method. The stability analysis of the model shows that the system is locally asymptotically stable at the disease-free equilibrium (DFE) \mathcal{E}_0 when $\mathcal{R}_0 < 1$. When $\mathcal{R}_0 > 1$, an endemic equilibrium \mathcal{E}^* exists and the system becomes locally asymptotically stable at \mathcal{E}^* under some conditions.

Keywords: Coronavirus(COVID-19); Caputo fractional derivative; reproduction number, next-generation matrix.

AMS Subject Classification: 92D30, 26A33, 37M05

1. INTRODUCTION

Coronavirus comprises a large family of viruses that are common in human beings as well animals (camels, cattle, cats, and bats). There are seven different strains of coronavirus namely 229E (alpha coronavirus), NL63 (alpha coronavirus), OC43 (beta coronavirus), HKU1 (beta coronavirus), MERS-CoV (the beta coronavirus that causes Middle East Respiratory Syndrome, or MERS), SARS-CoV (the beta coronavirus that causes severe acute respiratory syndrome, or SARS), SARS-CoV-2 (the novel coronavirus that causes coronavirus disease 2019, or COVID-19) for more details see [1].

Sometimes coronavirus from animals infect people and spread further via human to human transmission such as with MERS-CoV, SARS-CoV, and now with this COVID 19 (Corona disease 2019). The virus that causes COVID-19 is designated severe acute respiratory syndrome coronavirus 2 (SARS-CoV-2); previously, referred to as 2019-nCoV. Towards December 2019, this novel coronavirus was identified as a cause of upper and lower

¹ Department of Mathematics, Dr. Lankapalli Bullayya College, Resapuvanipalem, Visakhapatnam, 530013, India.

e-mail: khuddush89@gmail.com; ORCID: <https://orcid.org/0000-0002-1236-8334>.

* Corresponding author.

² Department of Applied Mathematics, College of Science and Technology, Andhra University, Visakhapatnam, 530003, India.

e-mail: rajendra92@rediffmail.com; ORCID: <https://orcid.org/0000-0001-8162-1391>.

§ Manuscript received: September 01, 2021; accepted: December 25, 2021.

TWMS Journal of Applied and Engineering Mathematics, Vol.13, No.4 © Işık University, Department of Mathematics, 2023; all rights reserved.

respiratory tract infections in Wuhan, a city in the Hubei province of China. It rapidly spread, resulting in an epidemic throughout China and then gradually spreading to other parts of the world in pandemic proportions. It has affected almost every continent in this world, except Antarctica. In February 2020, the world health organization designated the disease COVID-19, which stands for coronavirus disease 2019 (see [11]).

Several factors complicate the infection dynamics of COVID-19 and add challenges to the disease control. First, the origin of the infection is still uncertain, although it is widely speculated that wild animals such as bats, civets and minks are responsible for starting the epidemic [28]. Second, clinical evidence shows that the incubation period of this disease ranges from 2 to 14 days. During this period of time, infected individuals may not develop any symptoms and may not be aware of their infection, yet they are capable of transmitting the disease to other people [18]. Researchers suggested many mathematical models to analyze the dynamical behavior and spread of the novel virus which can help to predict the future situation and even control of the COVID-19 pandemic. In the analysis of mathematical models of coronavirus, the basic reproductive number has a significant role in describing the nonlinear dynamics of physical and biological engineering problems. The basic reproduction number indicates that COVID-19 has been continuously increasing or has been controlled. In [25], Wu et al., proposed SEIR model to describe the transmission dynamics, and estimated that the basic reproduction number for COVID-19 was about 2.68. In [17] Read et al. reported a value of 3.1 for the basic reproduction number based on data fitting of an SEIR model, using an assumption of Poisson-distributed daily time increments. In [23], Tang et al., proposed a deterministic compartmental model incorporating the clinical progression of the disease, the individual epidemiological status, and the intervention measures and estimated the reproduction number could be as high as 6.47, and reported that the quarantine and isolation can effectively reduce the control reproduction number and the transmission risk. More recently, Yang and wang [27] proposed a COVID-19 model with multiple transmission pathways in the infection dynamics, and emphasizes the role of the environmental reservoir in the transmission and spread of disease. Through data fitting, they obtained an estimate of basic reproduction number, $R_0 = 4.25$. The recent works on Covid-19 outbreak can be found in [3,4,12,21] and references therein.

The rest of the paper is organized in the following fashion. In Section 2, mathematical formulation of the model is discussed. In Section 3, useful lemmas and basic properties of the model are discussed. In Section 4, the basic reproduction number \mathcal{R}_0 is calculated using the next-generation matrix method and locally asymptotically stable at the disease-free equilibrium (DFE) \mathcal{E}_0 when $\mathcal{R}_0 < 1$. When $\mathcal{R}_0 > 1$, an endemic equilibrium \mathcal{E}^* exists and the system becomes locally asymptotically stable at \mathcal{E}^* under some conditions are discussed. Finally, as an application, numerical simulations are provided.

2. MATHEMATICAL FORMULATION OF THE MODEL

Following the work in [27], where the authors developed a framework for understanding the impact of environmental reservoir in the transmission and spread of disease, we use the same model with adding treatment compartment. We divide the total human population into five compartments: the susceptible S , the exposed E (individuals in this class are in the incubation period; they do not show symptoms but are still capable of infecting others), the infected I (individuals in this class have fully developed disease symptoms and can infect other people), the infected population in treatment T , the recovered R and the concentration of the coronavirus in the environment reservoir V_{19} . We study the following model which describes the transmission dynamics of the Covid-19 epidemic:

$$\left. \begin{aligned}
 {}^C\mathcal{D}_{0+}^a S(t) &= \pi - f(E)SE - g(I)SI - h(T)ST - \ell(V_{19})SV_{19} - \delta S \\
 {}^C\mathcal{D}_{0+}^a E(t) &= f(E)SE + g(I)SI + h(T)ST + \ell(V_{19})SV_{19} - [\epsilon + \delta]E \\
 {}^C\mathcal{D}_{0+}^a I(t) &= \epsilon E - [\tau + \eta + \delta]I \\
 {}^C\mathcal{D}_{0+}^a T(t) &= \tau I - [\varrho + \mu + \delta]T \\
 {}^C\mathcal{D}_{0+}^a R(t) &= \varrho T - \delta R \\
 {}^C\mathcal{D}_{0+}^a V_{19}(t) &= \alpha E + \beta I + \gamma T - \sigma V_{19},
 \end{aligned} \right\} \tag{C_{19}}$$

where ${}^C\mathcal{D}_{0+}^a$ denotes the Caputo fractional derivative of order $0 < a \leq 1$. The parameters of the model are described in Table 1.

TABLE 1. Parameter description and estimates for COVID-19 in Wuhan, China

PARAMETER SYMBOLS	PARAMETER DESCRIPTION	VALUE	SOURCE
π	the population influx	271.23 /day	[2]
δ	natural death rate of population	3.01×10^{-5} /day	[2]
$1/\epsilon$	incubation period	7 days	[22]
τ	the proportion of infective population who enter treatment	1.8887×10^{-7} /day	[23]
η	disease-related death rate of infective population who are not in treatment	0.01 /day	[2]
μ	disease-related death rate of infective population who are in treatment	1.7826×10^{-5} /day	[23]
ϱ	recovery rate of infective population in treatment	$\frac{1}{15}$ /day	[22]
α	rate of the exposed individuals contributing the coronavirus to the environmental reservoir	2.3 /person/day	[27]
β	rate of the infected individuals contributing the coronavirus to the environmental reservoir	0 /person/day	[27]
γ	rate of the infected individuals who are in treatment contributing the coronavirus to the environmental reservoir	0 /person/day	Assumed
σ	the removal rate of the coronavirus from the environment	01 per day	[8]

A schematic representation of the model (C_{19}) is shown in the following Fig. 1. The functions $f(E), g(I)$ and $h(T)$ represent the direct, human-to-human transmission rates between the exposed and susceptible individuals, between the infected and susceptible individuals, and between the infected population in the treatment and susceptible individuals, respectively, and the function $\ell(V_{19})$ represents the indirect, environment-to-human transmission rate. We assume that $f(E), g(I), h(T)$ and $\ell(V_{19})$ are all functions such that the higher values of E, I, T and V_{19} would motivate stronger control measures that could reduce the transmission rates.

We will investigate the system (C_{19}) subject to the initial conditions

$$S(0) = S_0 > 0, E(0) = E_0 > 0, I(0) = I_0 > 0,$$

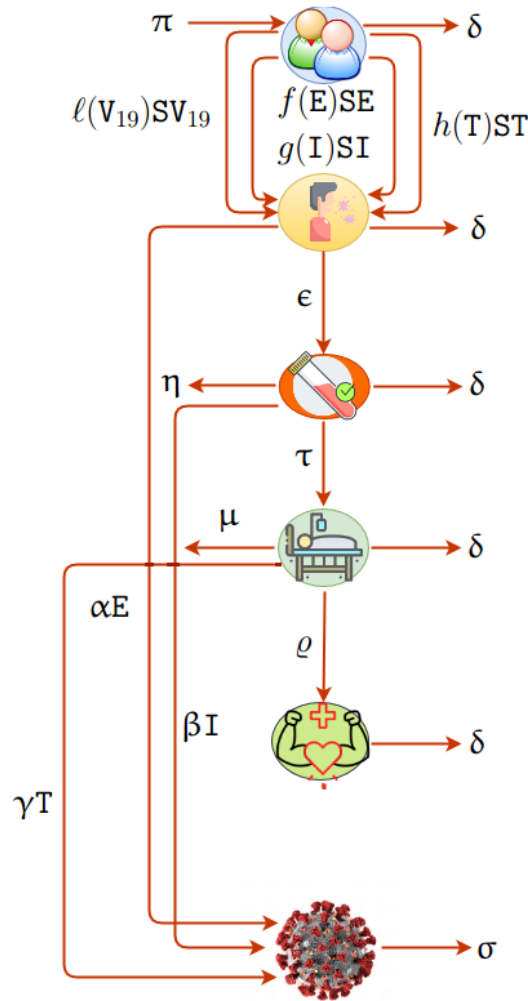


FIGURE 1. Schematic representation of the mathematical model (C_{19})

$$T(0) = T_0 > 0, R(0) = R_0 > 0, V_{19}(0) = V_0 > 0.$$

We make the following assumptions hold throughout the paper:

- (C_1) The functions $f(\mathbf{E})$, $g(\mathbf{I})$, $h(\mathbf{T})$ and $\ell(V_{19})$ are all positive.
- (C_2) The derivatives ${}^C\mathcal{D}_{0+}^a f(\mathbf{E}) \leq 0$, ${}^C\mathcal{D}_{0+}^a g(\mathbf{I}) \leq 0$, ${}^C\mathcal{D}_{0+}^a h(\mathbf{T}) \leq 0$ and ${}^C\mathcal{D}_{0+}^a \ell(V_{19}) \leq 0$.

In epidemiology, many works involving fractional order derivative have been done, and most of them are mainly concerned with SIR-type models with linear incidence rate [7, 9, 15, 20]. In [19] Saeedian et al., studied the memory effect of an SIR epidemic model using the Caputo fractional derivative and showed that the memory effect plays an essential role in the spreading of diseases. Therefore, our model generalizes [7, 9, 15, 19, 20].

3. BASIC PROPERTIES

In this section we provide some definitions, lemmas and basic properties of solutions of the model (C_{19}) .

Definition 3.1. [13, 16] The Riemann-Liouville fractional integral of order γ for a function f is defined as

$$\mathcal{I}_{0+}^{\gamma} f(t) := \frac{1}{\Gamma(\gamma)} \int_0^t (t-s)^{\gamma-1} f(s) ds, \quad a > 0.$$

Definition 3.2. [13, 16] For a function f given on the interval $[0, +\infty)$, the Caputo derivative of fractional order a for the function f continuous on $(0, +\infty)$ is defined as

$${}^{\mathcal{C}}\mathcal{D}_{0+}^a f(t) = \frac{1}{\Gamma(m-a)} \int_0^t (t-s)^{m-a-1} f^{(m)}(s) ds, \quad m = [a] + 1,$$

where $[a]$ denotes the integer part of a .

Lemma 3.1. [6] Consider the initial value problem of multi-order fractional order differential system in the Caputo sense,

$${}^{\mathcal{C}}\mathcal{D}_{0+}^{a_i} \mathbf{x}_i(t) = F_i(t, \mathbf{x}_1(t), \mathbf{x}_2(t), \dots, \mathbf{x}_n(t)), \quad 0 < a_i \leq 1, \quad t \in [0, \mathfrak{T}], \quad i = 1, 2, \dots, n, \quad (1)$$

with initial conditions,

$$\mathbf{x}_i(0) = c_i, \quad i = 1, 2, \dots, n. \quad (2)$$

Assume that the functions $F_i : [0, \mathfrak{T}] \times \mathbb{R}^n \rightarrow \mathbb{R}$, $i = 1, 2, \dots, n$ are continuous and satisfy Lipschitz conditions with respect to all their arguments except for the first. Then the initial value problem (1)-(2) admits a unique continuous solution.

Lemma 3.2. [14] Suppose that $\varphi(t) \in C[a, b]$ and ${}^{\mathcal{C}}\mathcal{D}_{a+}^{\alpha} \varphi(t) \in C[a, b]$ for $0 < \alpha \leq 1$,

$$\varphi(t) = \varphi(a) + \frac{1}{\Gamma(\alpha)} {}^{\mathcal{C}}\mathcal{D}_{a+}^{\alpha} \varphi(c) (t-a)^{\alpha}, \quad a < c < t, \quad \forall t \in (a, b].$$

Lemma 3.3. [14] Suppose that $\varphi(t) \in C[a, b]$ and ${}^{\mathcal{C}}\mathcal{D}_{a+}^{\alpha} \varphi(t) \in C[a, b]$ for $0 < \alpha \leq 1$. If ${}^{\mathcal{C}}\mathcal{D}_{a+}^{\alpha} \varphi(t) \geq 0 \forall t \in [a, b]$, then $\varphi(t)$ is nondecreasing for each $t \in [a, b]$. If ${}^{\mathcal{C}}\mathcal{D}_{a+}^{\alpha} \varphi(t) \leq 0 \forall t \in [a, b]$, then $\varphi(t)$ is nonincreasing for each $t \in [a, b]$.

Lemma 3.4. [16] Let a, b be positive real numbers and c be a complex number. The Laplace transform of

$$\mathbf{x}(t) = t^{b-1} \mathbf{E}_{a,b}(\pm ct^a),$$

where $\mathbf{E}_{a,b}(z)$ is the two parameter Mittag-Leffler function with parameters a and b , is given by

$$\hat{\mathbf{x}}(\lambda) = \frac{\lambda^{a-b}}{\lambda^a \mp c}. \quad (3)$$

In particular,

$$\mathcal{L}(t^a \mathbf{E}_{a,a+1}(-\delta t^a)) = \frac{\lambda^{-1}}{\lambda^a + \delta}, \quad (4)$$

$$\mathcal{L}(\mathbf{E}_{a,1}(-\delta t^a)) = \frac{\lambda^{a-1}}{\lambda^a + \delta}. \quad (5)$$

Lemma 3.5. [16] Let a and b be real numbers with $a < 2$. Then there exists a constant $\mathcal{C}_{\mathbf{E}}$ such that

$$|\mathbf{E}_{a,b}(z)| \leq \frac{\mathcal{C}_{\mathbf{E}}}{1 + |z|} \quad \text{for all } z \in \mathbb{C}.$$

Theorem 3.1. Let $\wp = \{(\mathbf{S}, \mathbf{E}, \mathbf{I}, \mathbf{T}, \mathbf{R}, \mathbf{V}_{19}) \in \mathbb{R}^6 : \max\{|\mathbf{S}|, |\mathbf{E}|, |\mathbf{I}|, |\mathbf{T}|, |\mathbf{R}|, |\mathbf{V}_{19}|\} < K\}$, where K is sufficiently large number. Further, suppose the following hold:

- (i) $|f(\mathbf{E}) - f(\bar{\mathbf{E}})| \leq |\mathbf{E} - \bar{\mathbf{E}}|$,
- (ii) $|g(\mathbf{I}) - g(\bar{\mathbf{I}})| \leq |\mathbf{I} - \bar{\mathbf{I}}|$,

- (iii) $|h(T) - h(\bar{T})| \leq |T - \bar{T}|,$
- (iv) $|\ell(V_{19}) - \ell(\bar{V}_{19})| \leq |V_{19} - \bar{V}_{19}|.$

Then the system (C_{19}) has a unique continuous solution on $[0, \mathfrak{T}] \times \wp$, where $\mathfrak{T} < +\infty$.

Proof. Let

$$\begin{aligned} F_1(t, S, E, I, T, R, V_{19}) &= \pi - f(E)SE - g(I)SI - h(T)ST - \ell(V_{19})SV_{19} - \delta S, \\ F_2(t, S, E, I, T, R, V_{19}) &= f(E)SE + g(I)SI + h(T)ST + \ell(V_{19})SV_{19} - [\epsilon + \delta]E, \\ F_3(t, S, E, I, T, R, V_{19}) &= \epsilon E - [\tau + \eta + \delta]I, \\ F_4(t, S, E, I, T, R, V_{19}) &= \tau I - [\rho + \mu + \delta]T, \\ F_5(t, S, E, I, T, R, V_{19}) &= \rho T - \delta R, \\ F_6(t, S, E, I, T, R, V_{19}) &= \alpha E + \beta I + \gamma T - \sigma V_{19}. \end{aligned}$$

Now, we show that each F_i satisfies the Lipschitz condition with respect to each of its arguments except for the first. For any $(S, E, I, T, R, V_{19}) \in \wp$ and $(\bar{S}, \bar{E}, \bar{I}, \bar{T}, \bar{R}, \bar{V}_{19}) \in \wp$, we have

$$\begin{aligned} &|F_1(S, E, I, T, R, V_{19}) - F_1(\bar{S}, \bar{E}, \bar{I}, \bar{T}, \bar{R}, \bar{V}_{19})| \\ &\leq |f(E)SE - f(\bar{E})\bar{S}\bar{E}| + |g(I)SI - g(\bar{I})\bar{S}\bar{I}| + |h(T)ST - h(\bar{T})\bar{S}\bar{T}| \\ &\quad + |\ell(V_{19})SV_{19} - \ell(\bar{V}_{19})\bar{S}\bar{V}_{19}| + \delta|S - \bar{S}| \\ &\leq |f(E) - f(\bar{E})||S||E| + f(\bar{E})|SE - \bar{S}\bar{E}| + |g(I) - g(\bar{I})||S||I| + g(\bar{I})|SI - \bar{S}\bar{I}| \\ &\quad + |h(T) - h(\bar{T})||S||T| + h(\bar{T})|ST - \bar{S}\bar{T}| + |\ell(V_{19}) - \ell(\bar{V}_{19})||S||V_{19}| \\ &\quad + \ell(\bar{V}_{19})|SV_{19} - \bar{S}\bar{V}_{19}| + \delta|S - \bar{S}|. \end{aligned}$$

Since

$$|SE - \bar{S}\bar{E}| \leq |S||E - \bar{E}| + |E||S - \bar{S}| \leq K(|E - \bar{E}| + |S - \bar{S}|). \tag{6}$$

Similarly, we can have

$$|SI - \bar{S}\bar{I}| \leq K(|I - \bar{I}| + |S - \bar{S}|), \tag{7}$$

$$|ST - \bar{S}\bar{T}| \leq K(|T - \bar{T}| + |S - \bar{S}|), \tag{8}$$

and

$$|SV_{19} - \bar{S}\bar{V}_{19}| \leq K(|V_{19} - \bar{V}_{19}| + |S - \bar{S}|). \tag{9}$$

Therefore, from the above inequalities (6)-(9), and (i), (ii), (iii) and (iv), we have

$$\begin{aligned} &|F_1(S, E, I, T, R, V_{19}) - F_1(\bar{S}, \bar{E}, \bar{I}, \bar{T}, \bar{R}, \bar{V}_{19})| \\ &\leq |f(E) - f(\bar{E})||S||E| + |g(I) - g(\bar{I})||S||I| + |h(T) - h(\bar{T})||S||T| + |\ell(V_{19}) - \ell(\bar{V}_{19})||S||V_{19}| \\ &\quad + [Kf(\bar{E}) + Kg(\bar{I}) + Kh(\bar{T}) + K\ell(\bar{V}_{19}) + \delta]|S - \bar{S}| \\ &\quad + Kf(\bar{E})|E - \bar{E}| + Kg(\bar{I})|I - \bar{I}| + Kh(\bar{T})|T - \bar{T}| + K\ell(\bar{V}_{19})|V_{19} - \bar{V}_{19}| \\ &\leq [Kf(\bar{E}) + Kg(\bar{I}) + Kh(\bar{T}) + K\ell(\bar{V}_{19}) + \delta]|S - \bar{S}| + [|S||E| + Kf(\bar{E})]|E - \bar{E}| \\ &\quad + [|S||I| + Kg(\bar{I})]|I - \bar{I}| + [|S||T| + Kh(\bar{T})]|T - \bar{T}| + [|S||V_{19}| + K\ell(\bar{V}_{19})]|V_{19} - \bar{V}_{19}| \\ &\leq [Kf(E_0) + Kg(I_0) + Kh(T_0) + K\ell(V_0) + \delta]|S - \bar{S}| + [K^2 + Kf(E_0)]|E - \bar{E}| \\ &\quad + [K^2 + Kg(I_0)]|I - \bar{I}| + [K^2 + Kh(T_0)]|T - \bar{T}| + [K^2 + K\ell(V_0)]|V_{19} - \bar{V}_{19}| \\ &\leq [K^2 + Kf(E_0) + Kg(I_0) + Kh(T_0) + K\ell(V_0) + \delta] \\ &\quad \times [|S - \bar{S}| + |E - \bar{E}| + |I - \bar{I}| + |T - \bar{T}| + |R - \bar{R}| + |V_{19} - \bar{V}_{19}|]. \end{aligned}$$

In similar fashion, we can check for the rest of the functions. Hence, $F_i(t, S, E, I, T, R, V_{19})$, $i = 1, 2, 3, 4, 5, 6$ satisfy the Lipschitz condition on \wp . Consequently, according to Lemma 3.1, the system (C_{19}) has a unique continuous solution on $[0, \mathfrak{T}] \times \wp$. \square

Theorem 3.2. *All solutions of the system (C_{19}) that start in \mathbb{R}_+^6 are nonnegative.*

Proof. From (C_{19}) , we have

$$\begin{aligned} {}^C\mathcal{D}_{0+}^a S(t)|_{S=0} &= \pi \geq 0, \\ {}^C\mathcal{D}_{0+}^a E(t)|_{E=0} &= g(I)SI + h(T)ST + \ell(V_{19})SV_{19} \geq 0, \\ {}^C\mathcal{D}_{0+}^a I(t)|_{I=0} &= \epsilon E \geq 0, \\ {}^C\mathcal{D}_{0+}^a T(t)|_{T=0} &= \tau I \geq 0, \\ {}^C\mathcal{D}_{0+}^a R(t)|_{R=0} &= \varrho T \geq 0, \\ {}^C\mathcal{D}_{0+}^a V_{19}(t)|_{V_{19}=0} &= \alpha E + \beta I + \gamma T \geq 0. \end{aligned}$$

Therefore, from Lemmas 3.1 and 3.2, all solutions of the system (C_{19}) that start in \mathbb{R}_+^6 are nonnegative. \square

Theorem 3.3. *The closed set*

$$\Omega = \left\{ (S, E, I, T, R, V_{19}) \in \mathbb{R}^6 : 0 \leq S + E + I + T + R \leq N, 0 \leq V_{19} \leq \hat{N}, \right. \\ \left. \text{where } N \geq \frac{\pi}{\delta} C_E, \hat{N} \geq \frac{(\alpha + \beta + \gamma)N}{\sigma} \hat{C}_E \right\}$$

is an attracting set of the system (C_{19}) , where C_E and \hat{C}_E are constants defined in Lemma 3.5.

Proof. Let $M(t) = S(t) + E(t) + I(t) + T(t) + R(t)$ and adding first five equations of (C_{19}) , we obtain

$$\begin{aligned} {}^C\mathcal{D}_{0+}^a M(t) &= \pi - \delta M(t) - \eta I - \mu T \\ &\leq \pi - \delta M(t). \end{aligned}$$

Applying Laplace transform, we have

$$\begin{aligned} \lambda^a \mathcal{L}(M(t)) - \lambda^{a-1} M(0) &\leq \pi \lambda^{-1} - \delta \mathcal{L}(M(t)), \\ \text{i.e., } (\lambda^a + \delta) \mathcal{L}(M(t)) &\leq \pi \lambda^{-1} + \lambda^{a-1} M(0). \end{aligned}$$

Now by using the Laplace transform properties (4) and (5), we get

$$\begin{aligned} \mathcal{L}(M(t)) &\leq \frac{\pi \lambda^{-1}}{\lambda^a + \delta} + \frac{\lambda^{a-1}}{\lambda^a + \delta} M(0) \\ &\leq \pi \mathcal{L}(t^a E_{a,a+1}(-\delta t^a)) + M(0) \mathcal{L}(E_{a,1}(-\delta t^a)). \end{aligned}$$

By inverse Laplace transform, we get

$$M(t) \leq \pi t^a E_{a,a+1}(-\delta t^a) + M(0) E_{a,1}(-\delta t^a).$$

Furthermore, by Lemma 3.5, we have

$$|M(t)| \leq \frac{\pi t^a C_E}{1 + \delta t^a} + \frac{M(0) C_E}{1 + \delta t^a}.$$

As $t \rightarrow \infty$, $|M(t)| \leq N$, where $N \geq \frac{\pi}{\delta} C_E$.

Next, from the last equation of the system (C_{19}) , we have

$$\begin{aligned} {}^C\mathcal{D}_{0+}^a \mathbf{V}_{19}(t) &= \alpha\mathbf{E} + \beta\mathbf{I} + \gamma\mathbf{T} - \sigma\mathbf{V}_{19} \\ &\leq (\alpha + \beta + \gamma)(\mathbf{S}(t) + \mathbf{E}(t) + \mathbf{I}(t) + \mathbf{T}(t) + \mathbf{R}(t)) - \sigma\mathbf{V}_{19} \\ &\leq (\alpha + \beta + \gamma)\mathbf{N} - \sigma\mathbf{V}_{19}. \end{aligned}$$

Similar to the above argument, we get $|\mathbf{V}_{19}(t)| \leq \hat{\mathbf{N}}$, where $\hat{\mathbf{N}} \geq \frac{(\alpha + \beta + \gamma)\mathbf{N}}{\sigma} \hat{\mathbf{C}}_{\mathbf{E}}$. Hence, the closed set Ω is attracting all solutions of the system (C_{19}) . \square

4. BASIC REPRODUCTION NUMBER

In this section, we derive the basic reproduction number by the general compartment method [24] and also using the notation of Van den Driessche and James Watmough [24]. The matrices \mathcal{F} and \mathcal{V} are respectively the rate of appearance of new infections and the rate of transfer from the group of infections. Also the matrices \mathcal{F} and \mathcal{V} stand for the new infection terms and the remaining terms respectively. The basic reproduction number is found by $\mathcal{R}_0 = \rho(\mathcal{F}\mathcal{V}^{-1})$ where $\rho(\mathcal{F}\mathcal{V}^{-1})$ is the spectral radius of the matrix $\mathcal{F}\mathcal{V}^{-1}$. The basic reproduction number \mathcal{R}_0 represents the average number of secondary infections caused by a single infectious in an entirely susceptible population during entire infection period. If $\mathcal{R}_0 < 1$, the number of infectives caused by a single infective less than 1. Then the infectious disease gradually dies out from the population. On the other hand if $\mathcal{R}_0 > 1$, the number of infectives caused by a single infective is greater than 1. Then there is a large outbreak of the infectious disease.

Let $\mathbf{x} = (\mathbf{S}, \mathbf{E}, \mathbf{I}, \mathbf{T}, \mathbf{R}, \mathbf{V}_{19})$, then the system (C_{19}) can be written as

$${}^C\mathcal{D}_{0+}^a \mathbf{x}(t) = \mathcal{F}(\mathbf{x}) - \mathcal{V}(\mathbf{x}),$$

where

$$\mathbf{x} = \begin{pmatrix} \mathbf{E} \\ \mathbf{I} \\ \mathbf{T} \\ \mathbf{R} \\ \mathbf{V}_{19} \\ \mathbf{S} \end{pmatrix}, \mathcal{F}(\mathbf{x}) = \begin{pmatrix} f(\mathbf{E})\mathbf{S}\mathbf{E} + g(\mathbf{I})\mathbf{S}\mathbf{I} + h(\mathbf{T})\mathbf{S}\mathbf{T} + \ell(\mathbf{V}_{19})\mathbf{S}\mathbf{V}_{19} \\ 0 \\ 0 \\ 0 \\ 0 \\ 0 \end{pmatrix},$$

and

$$\mathcal{V}(\mathbf{x}) = \begin{pmatrix} [\epsilon + \delta]\mathbf{E} \\ [\tau + \eta + \delta]\mathbf{I} - \epsilon\mathbf{E} \\ [\varrho + \mu + \delta]\mathbf{T} - \tau\mathbf{I} \\ \delta\mathbf{R} - \varrho\mathbf{T} \\ \sigma\mathbf{V}_{19} - (\alpha\mathbf{E} + \beta\mathbf{I} + \gamma\mathbf{T}) \\ \delta\mathbf{S} + f(\mathbf{E})\mathbf{S}\mathbf{E} + g(\mathbf{I})\mathbf{S}\mathbf{I} + h(\mathbf{T})\mathbf{S}\mathbf{T} + \ell(\mathbf{V}_{19})\mathbf{S}\mathbf{V}_{19} - \pi \end{pmatrix}.$$

Therefore,

$$\begin{aligned} \mathcal{F} = \text{Jacobian of } \mathcal{F} \text{ at disease-free equilibrium} &= \begin{pmatrix} f(0)\mathbf{S}_0 & g(0)\mathbf{S}_0 & h(0)\mathbf{S}_0 & \ell(0)\mathbf{S}_0 \\ 0 & 0 & 0 & 0 \\ 0 & 0 & 0 & 0 \\ 0 & 0 & 0 & 0 \end{pmatrix} \text{ and} \\ \mathcal{V} = \text{Jacobian of } \mathcal{V} \text{ at disease-free equilibrium} &= \begin{pmatrix} \epsilon + \delta & 0 & 0 & 0 \\ -\epsilon & \varpi_1 & 0 & 0 \\ 0 & -\tau & \varpi_2 & 0 \\ -\alpha & -\beta & -\gamma & \sigma \end{pmatrix}, \end{aligned}$$

where $\varpi_1 = \tau + \eta + \delta$ and $\varpi_2 = \varrho + \mu + \delta$. So, the next generation matrix for the system is

$$\mathcal{FV}^{-1} = \begin{pmatrix} A & B & C & D \\ 0 & 0 & 0 & 0 \\ 0 & 0 & 0 & 0 \\ 0 & 0 & 0 & 0 \end{pmatrix},$$

where

$$\begin{aligned} A &= \frac{f(0)\mathbf{S}_0}{\epsilon + \delta} + \frac{g(0)\mathbf{S}_0\epsilon}{(\epsilon + \delta)\varpi_1} + \frac{h(0)\mathbf{S}_0\epsilon\tau}{(\epsilon + \delta)\varpi_1\varpi_2} + \frac{\ell(0)\mathbf{S}_0(\varpi_1\varpi_2\alpha + \varpi_2\beta\epsilon + \epsilon\gamma\tau)}{(\epsilon + \delta)\varpi_1\varpi_2\sigma}, \\ B &= \frac{g(0)\mathbf{S}_0}{\varpi_1} + \frac{h(0)\mathbf{S}_0\tau}{\varpi_1\varpi_2} + \frac{\ell(0)\mathbf{S}_0(\varpi_2\beta + \gamma\tau)}{\varpi_1\varpi_2\sigma}, \\ C &= \frac{h(0)\mathbf{S}_0}{\varpi_2} + \frac{\ell(0)\mathbf{S}_0\gamma}{\varpi_2\sigma}, \\ D &= \frac{\ell(0)\mathbf{S}_0}{\sigma}, \end{aligned}$$

and the eigenvalues of \mathcal{FV}^{-1} are $0, 0, 0, A$. Therefore, the basic reproduction number

$$\begin{aligned} \mathcal{R}_0 &= \text{the spectral radius of } \mathcal{FV}^{-1}, \text{ i.e., } \rho(\mathcal{FV}^{-1}) \\ &= \text{the dominant eigenvalue of } \mathcal{FV}^{-1} \\ &= A \\ &= \frac{f(0)\mathbf{S}_0}{\epsilon + \delta} + \frac{g(0)\mathbf{S}_0\epsilon}{(\epsilon + \delta)\varpi_1} + \frac{h(0)\mathbf{S}_0\epsilon\tau}{(\epsilon + \delta)\varpi_1\varpi_2} + \frac{\ell(0)\mathbf{S}_0(\varpi_1\varpi_2\alpha + \varpi_2\beta\epsilon + \epsilon\gamma\tau)}{(\epsilon + \delta)\varpi_1\varpi_2\sigma} \\ &:= \mathcal{R}_1 + \mathcal{R}_2 + \mathcal{R}_3 + \mathcal{R}_4, \end{aligned}$$

which provides a quantification of the disease risk. The first three parts $\mathcal{R}_1, \mathcal{R}_2$ and \mathcal{R}_3 measure the contributions from the human-to-human transmission routes i.e., exposed-to-susceptible, infected-to-susceptible and infected persons in treatment-to-susceptible respectively, and the third part \mathcal{R}_4 represents the contribution from the environment-to-human transmission route. These four transmission modes collectively shape the overall infection risk for the COVID-19 outbreak.

Theorem 4.1. *The disease-free equilibrium $\mathcal{E}_0(\pi/\delta, 0, 0, 0, 0, 0)$ of the model (C_{19}) is globally asymptotically stable if $\mathcal{R}_0 < 1$.*

Proof. Let $\mathbf{U} = (\mathbf{E}, \mathbf{I}, \mathbf{T}, \mathbf{V}_{19})^T$. Then from (C_{19}) , we have

$$\begin{aligned} {}^c\mathcal{D}_{0+}^a \mathbf{U} &= \begin{pmatrix} f(\mathbf{E})\mathbf{S} & g(\mathbf{I})\mathbf{S} & h(\mathbf{T})\mathbf{S} & \ell(\mathbf{V}_{19})\mathbf{S} \\ 0 & 0 & 0 & 0 \\ 0 & 0 & 0 & 0 \\ 0 & 0 & 0 & 0 \end{pmatrix} \mathbf{U} - \begin{pmatrix} \epsilon + \delta & 0 & 0 & 0 \\ -\epsilon & \varpi_1 & 0 & 0 \\ 0 & -\tau & \varpi_2 & 0 \\ -\alpha & -\beta & -\gamma & \sigma \end{pmatrix} \mathbf{U} \\ &\leq (\mathcal{F} - \mathcal{V})\mathbf{U}. \end{aligned}$$

After certain calculations, we obtained that $\rho(\mathcal{FV}^{-1}) = \rho(\mathcal{V}^{-1}\mathcal{F}) = \mathcal{R}_0$.

Next, let $\vartheta = (f(0), g(0), h(0), \ell(0))$. Then it can be seen that ϑ is the left eigenvector of $\mathcal{V}^{-1}\mathcal{F}$ corresponding to the eigenvalue \mathcal{R}_0 . That is $\vartheta(\mathcal{V}^{-1}\mathcal{F}) = \mathcal{R}_0\vartheta$.

Consider the Lyapunov function,

$$\mathcal{L} = \vartheta\mathcal{V}^{-1}\mathbf{U}.$$

Then by differentiating, we get

$${}^c\mathcal{D}_{0+}^a \mathcal{L} = \vartheta\mathcal{V}^{-1}({}^c\mathcal{D}_{0+}^a \mathbf{U}) \leq \vartheta\mathcal{V}^{-1}(\mathcal{F} - \mathcal{V})\mathbf{U} = \vartheta(\mathcal{R}_0 - 1)\mathbf{U}. \tag{10}$$

If $\mathcal{R}_0 < 1$, the equality ${}^C\mathcal{D}_{0+}^a \mathcal{L} = 0$ implies from (10) that $\vartheta U = 0$. Since components of ϑ are positive, it follows that $E = I = T = V_{19} = 0$. So, when $\mathcal{R}_0 < 1$, we have $S = S_0$, and $E = I = T = V_{19} = 0$. Thus, the invariant set on which ${}^C\mathcal{D}_{0+}^a \mathcal{L} = 0$ contains only the point \mathcal{E}_0 .

If $\mathcal{R}_0 = 1$, then ${}^C\mathcal{D}_{0+}^a \mathcal{L} = 0$ gives

$$\begin{aligned} & \left[\frac{f(E)S}{S_0} + \frac{g(I)\eta}{\varpi_1} + \frac{h(T)\eta\tau}{\varpi_1\varpi_2} + \frac{\ell(V_{19})(\varpi_1\varpi_2\alpha + \varpi_2\beta\eta + \eta\gamma\tau)}{\varpi_1\varpi_2\sigma} - \frac{\eta + \delta}{S_0} \right] E \\ & + \left[\frac{g(I)S}{S_0} - g(0) \right] I + \left[\frac{h(T)S}{S_0} - h(0) \right] T + \left[\frac{\ell(V_{19})S}{S_0} - \ell(0) \right] V_{19} = 0. \end{aligned}$$

Since $\frac{g(I)S}{S_0} \leq g(0)$, $\frac{h(T)S}{S_0} \leq h(0)$, $\frac{\ell(V_{19})S}{S_0} \leq \ell(0)$ and

$$\frac{f(E)S}{S_0} + \frac{g(I)\eta}{\varpi_1} + \frac{h(T)\eta\tau}{\varpi_1\varpi_2} + \frac{\ell(V_{19})(\varpi_1\varpi_2\alpha + \varpi_2\beta\eta + \eta\gamma\tau)}{\varpi_1\varpi_2\sigma} - \frac{\eta + \delta}{S_0} \leq \frac{\eta + \delta}{S_0} [\mathcal{R}_0 - 1] = 0,$$

it follows that $E = I = T = V_{19} = 0$ or $f(E) = f(0)$, $g(I) = g(0)$, $h(T) = h(0)$, $\ell(V_{19}) = \ell(0)$ and $S = S_0$. From the above arguments, we conclude that the largest invariant set of $\{(S, E, I, T, R, V_{19}) : {}^C\mathcal{D}_{0+}^a \mathcal{L} = 0\}$ is the singleton $\{\mathcal{E}_0\}$. Consequently, from Lemma 4.6 in [10], \mathcal{E}_0 is globally asymptotically stable. \square

Theorem 4.2. *If $\mathcal{R}_0 > 1$, then the endemic equilibrium \mathcal{E}^* of the model (C₁₉) is globally asymptotically stable.*

Proof. Let

$$\mathcal{L}(y) = y^* \varphi(y),$$

where $\varphi(y) = y - 1 - \ln(y)$, $y > 0$. It is clear that $\varphi(y) \geq 0$. Then by Lemma 3.1 in [5], we have

$$\begin{aligned} {}^C\mathcal{D}_{0+}^a \mathcal{L}(S) &= \left[\frac{S - S^*}{S} \right] {}^C\mathcal{D}_{0+}^a S \\ &\leq \left[\frac{S - S^*}{S} \right] \left[f^*(E)S^*E^* - f(E)SE + g^*(I)S^*I^* - g(I)SI + h^*(T)S^*T^* - h(T)ST \right. \\ &\quad \left. + \ell^*(V_{19})S^*V_{19}^* - \ell(V_{19})SV_{19} \right] \\ &\leq f^*(E)S^*E^* \left[\frac{S - S^*}{S} + \frac{S - S^*}{S} \frac{f(E)SE}{f^*(E)S^*E^*} \right] + g^*(I)S^*I^* \left[\frac{S - S^*}{S} + \frac{S - S^*}{S} \frac{g(I)SI}{g^*(I)S^*I^*} \right] \\ &\quad + h^*(T)S^*T^* \left[\frac{S - S^*}{S} + \frac{S - S^*}{S} \frac{h(T)ST}{h^*(T)S^*T^*} \right] + \ell^*(E)S^*E^* \left[\frac{S - S^*}{S} + \frac{S - S^*}{S} \frac{\ell(V_{19})SV_{19}}{\ell^*(V_{19})S^*V_{19}^*} \right] \\ &\leq f^*(E)S^*E^* \left[1 - \frac{S^*}{S} - \frac{f(E)SE}{f^*(E)S^*E^*} + \frac{f(E)E}{f^*(E)E^*} \right] + g^*(I)S^*I^* \left[1 - \frac{S^*}{S} - \frac{g(I)SI}{g^*(I)S^*I^*} + \frac{g(I)I}{g^*(I)I^*} \right] \\ &\quad + h^*(T)S^*T^* \left[1 - \frac{S^*}{S} - \frac{h(T)ST}{h^*(T)S^*T^*} + \frac{h(T)T}{h^*(T)T^*} \right] \\ &\quad + \ell^*(V_{19})S^*V_{19}^* \left[1 - \frac{S^*}{S} - \frac{\ell(V_{19})SV_{19}}{\ell^*(V_{19})S^*E^*} + \frac{\ell(V_{19})V_{19}}{\ell^*(V_{19})V_{19}^*} \right], \end{aligned}$$

and

$$\begin{aligned}
 {}^c\mathcal{D}_{0+}^a \mathcal{L}(\mathbf{E}) &= \left[\frac{\mathbf{E} - \mathbf{E}^*}{\mathbf{E}} \right] {}^c\mathcal{D}_{0+}^a \mathbf{E} \\
 &= \left[\frac{\mathbf{E} - \mathbf{E}^*}{\mathbf{E}} \right] \left[f(\mathbf{E})\mathbf{S}\mathbf{E} + g(\mathbf{I})\mathbf{S}\mathbf{I} + h(\mathbf{T})\mathbf{S}\mathbf{T} + \ell(\mathbf{V}_{19})\mathbf{S}\mathbf{V}_{19} - [\epsilon + \delta]\mathbf{E} \right] \\
 &\leq f^*(\mathbf{E})\mathbf{S}^*\mathbf{E}^* \left[1 - \frac{\mathbf{E}}{\mathbf{E}^*} + \frac{f(\mathbf{E})\mathbf{S}\mathbf{E}}{f^*(\mathbf{E})\mathbf{S}^*\mathbf{E}^*} - \frac{f(\mathbf{E})\mathbf{S}}{f^*(\mathbf{E})\mathbf{S}^*} \right] \\
 &\quad + g^*(\mathbf{I})\mathbf{S}^*\mathbf{I}^* \left[1 - \frac{\mathbf{E}}{\mathbf{E}^*} - \frac{g(\mathbf{I})\mathbf{S}\mathbf{E}^*\mathbf{I}}{g^*(\mathbf{I})\mathbf{S}^*\mathbf{E}\mathbf{I}^*} + \frac{g(\mathbf{I})\mathbf{S}\mathbf{I}}{g^*(\mathbf{I})\mathbf{S}^*\mathbf{I}^*} \right] \\
 &\quad + h^*(\mathbf{T})\mathbf{S}^*\mathbf{T}^* \left[1 - \frac{\mathbf{E}}{\mathbf{E}^*} - \frac{h(\mathbf{T})\mathbf{S}\mathbf{E}^*\mathbf{T}}{h^*(\mathbf{T})\mathbf{S}^*\mathbf{E}\mathbf{T}^*} + \frac{h(\mathbf{T})\mathbf{S}\mathbf{T}}{h^*(\mathbf{T})\mathbf{S}^*\mathbf{T}^*} \right] \\
 &\quad + \ell^*(\mathbf{V}_{19})\mathbf{S}^*\mathbf{V}_{19}^* \left[1 - \frac{\mathbf{E}}{\mathbf{E}^*} - \frac{\ell(\mathbf{V}_{19})\mathbf{S}\mathbf{V}_{19}\mathbf{E}^*}{\ell^*(\mathbf{V}_{19})\mathbf{S}^*\mathbf{V}_{19}^*\mathbf{E}} + \frac{\ell(\mathbf{V}_{19})\mathbf{V}_{19}\mathbf{S}}{\ell^*(\mathbf{V}_{19})\mathbf{V}_{19}^*\mathbf{S}^*} \right].
 \end{aligned}$$

Now adding above two inequalities and using the same technique of [27], we obtain

$$\begin{aligned}
 {}^c\mathcal{D}_{0+}^a \mathcal{L}(\mathbf{S}) + {}^c\mathcal{D}_{0+}^a \mathcal{L}(\mathbf{E}) &\leq g^*(\mathbf{I})\mathbf{I}^*\mathbf{S}^* \left[\frac{\mathbf{I}}{\mathbf{I}^*} - \frac{\mathbf{E}}{\mathbf{E}^*} - \ln \left(\frac{\mathbf{I}}{\mathbf{I}^*} \right) + \ln \left(\frac{\mathbf{E}}{\mathbf{E}^*} \right) \right] \\
 &\quad + h^*(\mathbf{T})\mathbf{T}^*\mathbf{S}^* \left[\frac{\mathbf{T}}{\mathbf{T}^*} - \frac{\mathbf{E}}{\mathbf{E}^*} - \ln \left(\frac{\mathbf{T}}{\mathbf{T}^*} \right) + \ln \left(\frac{\mathbf{E}}{\mathbf{E}^*} \right) \right] \\
 &\quad + \ell^*(\mathbf{V}_{19})\mathbf{V}_{19}^*\mathbf{S}^* \left[\frac{\mathbf{V}_{19}}{\mathbf{V}_{19}^*} - \frac{\mathbf{E}}{\mathbf{E}^*} - \ln \left(\frac{\mathbf{V}_{19}}{\mathbf{V}_{19}^*} \right) + \ln \left(\frac{\mathbf{E}}{\mathbf{E}^*} \right) \right].
 \end{aligned}$$

Similarly, we have

$$\begin{aligned}
 {}^c\mathcal{D}_{0+}^a \mathcal{L}(\mathbf{I}) &\leq \epsilon\mathbf{E}^* \left[\frac{\mathbf{E}}{\mathbf{E}^*} - \frac{\mathbf{I}}{\mathbf{I}^*} + \ln \left(\frac{\mathbf{I}}{\mathbf{I}^*} \right) - \ln \left(\frac{\mathbf{E}}{\mathbf{E}^*} \right) \right], \\
 {}^c\mathcal{D}_{0+}^a \mathcal{L}(\mathbf{T}) &\leq \tau\mathbf{I}^* \left[\frac{\mathbf{I}}{\mathbf{I}^*} - \frac{\mathbf{T}}{\mathbf{T}^*} + \ln \left(\frac{\mathbf{T}}{\mathbf{T}^*} \right) - \ln \left(\frac{\mathbf{I}}{\mathbf{I}^*} \right) \right], \\
 {}^c\mathcal{D}_{0+}^a \mathcal{L}(\mathbf{V}_{19}) &\leq \alpha\mathbf{E}^* \left[\frac{\mathbf{E}}{\mathbf{E}^*} - \frac{\mathbf{V}_{19}}{\mathbf{V}_{19}^*} + \ln \left(\frac{\mathbf{V}_{19}}{\mathbf{V}_{19}^*} \right) - \ln \left(\frac{\mathbf{E}}{\mathbf{E}^*} \right) \right] \\
 &\quad + \beta\mathbf{I}^* \left[\frac{\mathbf{I}}{\mathbf{I}^*} - \frac{\mathbf{V}_{19}}{\mathbf{V}_{19}^*} + \ln \left(\frac{\mathbf{V}_{19}}{\mathbf{V}_{19}^*} \right) - \ln \left(\frac{\mathbf{I}}{\mathbf{I}^*} \right) \right] \\
 &\quad + \gamma\mathbf{T}^* \left[\frac{\mathbf{T}}{\mathbf{T}^*} - \frac{\mathbf{V}_{19}}{\mathbf{V}_{19}^*} + \ln \left(\frac{\mathbf{V}_{19}}{\mathbf{V}_{19}^*} \right) - \ln \left(\frac{\mathbf{T}}{\mathbf{T}^*} \right) \right].
 \end{aligned}$$

Finally, we consider a Lyapunov function \mathcal{F} for the system (C_{19}) as

$$\mathcal{L}_{\mathcal{F}} = \mathcal{L}(\mathbf{S}) + \mathcal{L}(\mathbf{E}) + \kappa_1\mathcal{L}(\mathbf{I}) + \kappa_2\mathcal{L}(\mathbf{T}) + \kappa_3\mathcal{L}(\mathbf{V}_{19}),$$

where

$$\begin{aligned}
 \kappa_1 &= \frac{g^*(\mathbf{I})\mathbf{I}^*\mathbf{S}^*}{\epsilon\mathbf{E}^*} + \frac{h^*(\mathbf{T})\mathbf{T}^*\mathbf{S}^*}{\epsilon\mathbf{E}^*} + \frac{(\tau + \varpi_2\beta)\ell^*(\mathbf{V}_{19})\mathbf{V}_{19}^*\mathbf{S}^*}{(\alpha\varpi_1\varpi_2 + \beta\epsilon\varpi_2 + \gamma\tau\epsilon)\mathbf{E}^*}, \\
 \kappa_2 &= \frac{h^*(\mathbf{T})\mathbf{T}^*\mathbf{S}^*}{\tau\mathbf{I}^*} + \frac{\ell^*(\mathbf{V}_{19})\mathbf{V}_{19}^*\mathbf{S}^*\varpi_1}{(\alpha\varpi_1\varpi_2 + \beta\epsilon\varpi_2 + \gamma\tau\epsilon)\mathbf{E}^*}, \\
 \kappa_3 &= \frac{\ell^*(\mathbf{V}_{19})\mathbf{V}_{19}^*\mathbf{S}^*\varpi_1\varpi_2}{(\alpha\varpi_1\varpi_2 + \beta\epsilon\varpi_2 + \gamma\tau\epsilon)\mathbf{E}^*}.
 \end{aligned}$$

TABLE 2. Estimates for maximum values of the transmission rates

PARAMETER SYMBOLS	VALUE	SOURCE
$f(\mathbf{E}_0)$	3.11×10^{-8} /person/day	[23]
$g(\mathbf{I}_0)$	0.02×10^{-8} /person/day	[23]
$h(\mathbf{T}_0)$	0.13×10^{-8} /person/day	[23]
$\ell(\mathbf{V}_0)$	1.03×10^{-8} /person/day	[27]
r	1.01×10^{-4}	[27]

Then, it is clear from the definition of $\mathcal{L}(y)$ that $\mathcal{L}_{\mathcal{F}} \geq 0$ and

$$\begin{aligned}
 {}^c\mathcal{D}_{0+}^a \mathcal{L}_{\mathcal{F}} \leq & \left[g^*(\mathbf{I})\mathbf{I}^*\mathbf{S}^* + h^*(\mathbf{T})\mathbf{T}^*\mathbf{S}^* + \ell^*(\mathbf{V}_{19})\mathbf{V}_{19}^*\mathbf{S}^* - \kappa_1\epsilon\mathbf{E}^* - \kappa_3\alpha\mathbf{E}^* \right] \left[\ln \left(\frac{\mathbf{E}}{\mathbf{E}^*} \right) - \frac{\mathbf{E}}{\mathbf{E}^*} \right] \\
 & + \left[g^*(\mathbf{I})\mathbf{I}^*\mathbf{S}^* - \kappa_1\epsilon\mathbf{E}^* + \kappa_2\tau\mathbf{I}^* + \kappa_3\beta\mathbf{I}^* \right] \left[\frac{\mathbf{I}}{\mathbf{I}^*} - \ln \left(\frac{\mathbf{I}}{\mathbf{I}^*} \right) \right] \\
 & + \left[h^*(\mathbf{T})\mathbf{T}^*\mathbf{S}^* - \kappa_2\tau\mathbf{I}^* + \kappa_3\gamma\mathbf{T}^* \right] \left[\frac{\mathbf{T}}{\mathbf{T}^*} - \ln \left(\frac{\mathbf{T}}{\mathbf{T}^*} \right) \right] \\
 & + \left[\ell^*(\mathbf{V}_{19})\mathbf{V}_{19}^*\mathbf{S}^* - \kappa_3(\alpha\mathbf{E}^* + \beta\mathbf{I}^* + \gamma\mathbf{T}^*) \right] \left[\frac{\mathbf{V}_{19}}{\mathbf{V}_{19}^*} - \ln \left(\frac{\mathbf{V}_{19}}{\mathbf{V}_{19}^*} \right) \right] \\
 \leq & 0.
 \end{aligned}$$

Therefore, ${}^c\mathcal{D}_{0+}^a \mathcal{L}_{\mathcal{F}} \leq 0$, if and only if $(\mathbf{S}, \mathbf{E}, \mathbf{I}, \mathbf{T}, \mathbf{V}_{19}) = (\mathbf{S}^*, \mathbf{E}^*, \mathbf{I}^*, \mathbf{T}^*, \mathbf{V}_{19}^*)$. Furthermore, the largest invariant set of $\{(\mathbf{S}, \mathbf{E}, \mathbf{I}, \mathbf{T}, \mathbf{V}_{19}) \in \mathbb{R}^5 : {}^c\mathcal{D}_{0+}^a \mathcal{L}_{\mathcal{F}} = 0\}$ is only the singleton $\{\mathcal{E}^*\}$. Hence, by LaSalle’s invariance principle [10], \mathcal{E}^* is globally asymptotically stable. \square

5. NUMERICAL SIMULATIONS

We now apply our model to study the COVID-19 outbreak in the city of Wuhan, based on sources available by WHO and [8, 22, 23, 27]. We implement our model and conduct numerical simulation for an epidemic period starting from Jan 23-July 27, 2021.

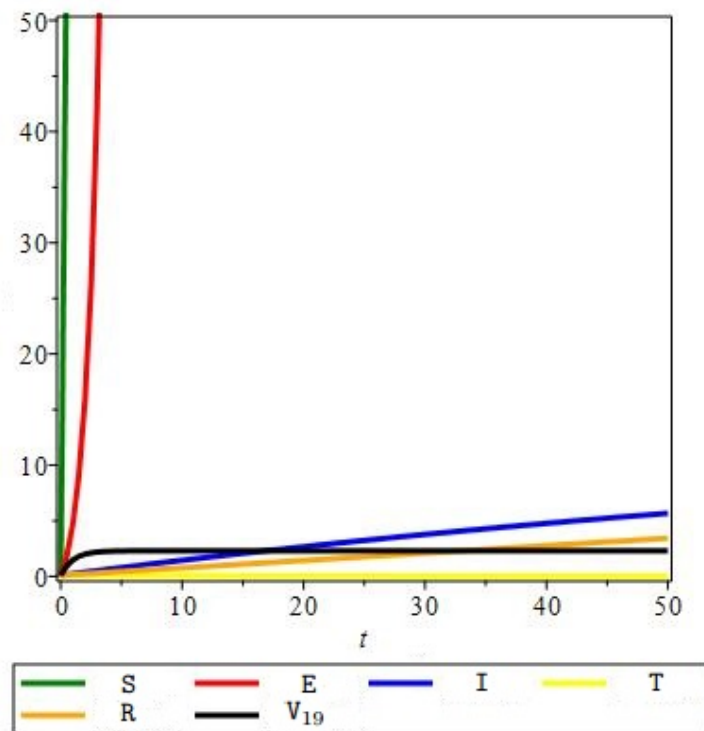
To conduct the numerical simulation, we consider the following functions(see [26]) for the four transmission rates in our model.

$$f(\mathbf{E}) = \frac{f(\mathbf{E}_0)}{1 + r\mathbf{E}}, \quad g(\mathbf{I}) = \frac{g(\mathbf{I}_0)}{1 + r\mathbf{I}}, \quad h(\mathbf{T}) = \frac{h(\mathbf{T}_0)}{1 + r\mathbf{T}}, \quad \ell(\mathbf{V}_{19}) = \frac{\ell(\mathbf{V}_0)}{1 + r\mathbf{V}_{19}},$$

where the positive constants $f(\mathbf{E}_0), g(\mathbf{I}_0), h(\mathbf{T}_0)$ and $\ell(\mathbf{V}_0)$ denote the maximum values of these transmission rates, and r is a positive constant and whose value are listed in the Table 2. From the tabular values, we get

$$\mathcal{R}_1 = 1.961273503, \mathcal{R}_2 = 0.1796372041, \mathcal{R}_3 = 0.3305611304 \times 10^{-5}, \mathcal{R}_4 = 1.493973290.$$

Therefore, the basic reproduction number $\mathcal{R}_0 = 3.634887303$. Among these four components, the largest one \mathcal{R}_1 comes from the exposed-to-susceptible transmission, since exposed individuals show no symptoms and can easily spread the infection to other people with close contact, often in an unconscious manner. The smallest component \mathcal{R}_3 comes from infected persons in treatment-to-susceptible and \mathcal{R}_2 comes from the infected-to-susceptible transmission, possibly due to the strict isolation policy on the symptomatic infected individuals. In addition, we observe that $\mathcal{R}_4 = 1.493973290$, showing a significant contribution from the environmental reservoir toward the overall infection risk.

FIGURE 2. Dynamics of model (C_{19})

6. CONCLUSION

In this study, the nonlinear mathematical model was proposed and analyzed to understand the dynamics of the COVID-19 pandemic. The equilibrium point relating to the formulated model was computed. Using the next generation matrix approach, the basic reproduction number denoted as relating to the model was also computed. Moreover, this study also showed that if the \mathcal{R}_0 is denoted as $\mathcal{R}_0 < 1$, then the pandemic will die out. However, if $\mathcal{R}_0 > 1$, then the pandemic will remain in the population. Additionally, the global asymptotical stability of the disease-free and endemic equilibrium points has been proved. Numerical simulations were carried out to support the model analysis. The real data were also fitted to the model for predicting the infected population cases in real life.

Acknowledgement. The authors would like to thank the referees for their valuable suggestions and comments for the improvement of the paper.

REFERENCES

- [1] National Center for Immunization and Respiratory Diseases (NCIRD), Division of Viral Diseases.
- [2] The government of Wuhan homepage. Available from: <http://english.wh.gov.cn/>.
- [3] Boutiara, A., Matar, M. M., Kaabar, M. K. A., Martinez, F., Etemad, S., Rezapour, S., (2021), Some qualitative analysis of neutral functional delay differential equation with generalized Caputo operator, J. Function Spaces. <http://doi.org/10.1155/2021/9993177>
- [4] Bozkurt, F., Yousef, A., Baleanu, D., Alzabut, J., (2021), A mathematical model of the evolution and spread of pathogenic coronaviruses from natural host to human host, Chaos Solitons Fractals, 138, Article ID 109931. <https://doi.org/10.1016/j.chaos.2020.109931>
- [5] De-Leon, C. V., (2015), Volterra-type Lyapunov functions for fractional order epidemic systems, Commun. Nonlinear Sci. Numer. Simul., 24, 75-85.

- [6] Diethelm, K., (2010), The analysis of fractional differential equations, Berlin, Springer-Verlag.
- [7] Dos Santos, J. P. C., Monteiro, E., Vieira, G. B., (2017), Global stability of fractional SIR epidemic model, Proc. Ser. Braz. Soc. Comput. Appl. Math., 5 (1), 1-7.
- [8] Geller, C., Varbanov, M., Duval, R. E., (2012), Human coronaviruses: Insights into environmental resistance and its influence on the development of new antiseptic strategies, Viruses, 4, 3044-3068.
- [9] Guo, Y., (2017), The stability of the positive solution for a fractional SIR model, Int. J. Biomath., 1, 1-14.
- [10] Huo, J., Zhao, H., Zhu, L., (2015), The effect of vaccines on backward bifurcation in a fractional order HIV model, Nonlinear Anal. Real World Appl., 26, 289-305.
- [11] Joseph, T, Moslehi, M. A, (2020), International pulmonologists consensus on COVID-19. <https://www.unah.edu.hk/dmsdocument/9674-consenso-internacional-de-neumologos-sobre-covid-19-version-ingles>.
- [12] Khan, T., Ullah, R., Zaman, G., Alzabut, J., (2021), A mathematical model for the dynamics of SARS-CoV-2 virus using the Caputo-Fabrizio operator, Mathematical Biosciences and Engineering, 18 (5), 6095-116.
- [13] Kilbas, A. A., Srivastava, H. M., Trujillo, J. J., (2006), Theory and applications of fractional differential equations, North-Holland Mathematics Studies 204, Elsevier Science B. V., Amsterdam.
- [14] Odibat, Z. M., Shawagfeh, N. T., (2007), Generalized Taylor's formula, Appl. Math. Comp., 186 (1), 286-293.
- [15] Okyere, E., Oduro, F. T., Amponsah, S. K., Dontwi, I. K., Frempong, N. K., (2016), Fractional order SIR model with constant population, Br. J. Math. Comput. Sci., 14 (2), 1-12.
- [16] Podlubny, I., (1998), Fractional differential equations: An introduction to fractional derivatives, fractional differential equations, to methods of their solution and some of their applications, Academic Press, San Diego, 198.
- [17] Read, J. M., Bridgen, J. R. E., Cummings, D. A. T., Ho, A., Jewell, C. P., (2020), Novel coronavirus 2019-nCoV: early estimation of epidemiological parameters and epidemic predictions, medRxiv.
- [18] Rothe, C., Schunk, M., Sothmann, P., Bretzel, G., Froeschl, G., Wallrauch, C., et al., (2020), Transmission of 2019-nCoV Infection from an asymptomatic contact in Germany, N. Engl. J. Med.
- [19] Saeedian, M., Khalighi, M., Tafreshi, N. A., Jafari, G. R., Ausloos, M., (2017), Memory effects on epidemic evolution: the susceptible-infected-recovered epidemic model. Phys. Rev. E 95, 022409.
- [20] Saka, H. A. A. E., (2013), The fractional order SIR and SIRS epidemic models with variable population size, Math. Sci. Lett., 2, 195-200.
- [21] Selvam, A. G., Alzabut, J., Vianny, D. A., Jacintha, M., Yousef, F. B., (2021), Modeling and stability analysis of the spread of novel coronavirus disease COVID-19, I. J. Biomath., 14 (5), 215005.
- [22] Spencer, J. A., Shutt, D. P., Moser, S. K., Clegg, H., Wearing, J., Mukundan, H., et al., (2020), Epidemiological parameter review and comparative dynamics of influenza, respiratory syncytial virus, rhinovirus, human coronavirus, and adenovirus, medRxiv.
- [23] Tang, B., Wang, X., Li, Q., Bragazzi, N. L., Tang, S., Xiao, Y., et al., (2020), Estimation of the transmission risk of 2019-nCoV and its implication for public health interventions, J. Clin. Med., 9, 462.
- [24] Van den Driessche, P., Watmough, J., (2002), Reproductive numbers and sub-threshold endemic equilibria for compartmental models of disease transmission, Math. Biosci., 180, 22-48.
- [25] Wu, J. T., Leung, K., Leung, G. M., (2020), Nowcasting and forecasting the potential domestic and international spread of the 2019-nCoV outbreak originating in Wuhan, China: a modelling study, Lancet, 395, 689-697.
- [26] Yang, C., Wang, J., (2019), A cholera transmission model incorporating the impact of medical resources, Math. Biosci. Eng., 16 5226-5246.
- [27] Yang, C., Wang, J., A mathematical model for the novel coronavirus epidemic in Wuhan, China, Math. Biosci. Eng., 17 (3), 2708-2724.
- [28] Zhou, P., Yang, X. L., Wang, X. G., Hu, B., Zhang, L., Zhang, W., et al., (2020), Discovery of a novel coronavirus associated with the recent pneumonia outbreak in humans and its potential bat origin, bioRxiv.

Mahammad Khuddush for the photography and short autobiography, see TWMS J. App. and Eng. Math. V.12, N.1.

Kapula Rajendra Prasad for the photography and short autobiography, see TWMS J. App. and Eng. Math. V.12, N.1.
